Detonation-driven-shock wave interactions with perforated plates

1 author:

Hossein Zare-Behtash
University of Glasgow
121 PUBLICATIONS   **1,421** CITATIONS

SEE PROFILE

Detonation Driven Shock Wave Interactions
with Perforated Plates

H. Zare-Behtash, N. Gongora-Orozco, and K. Kontis*

School of Mechanical, Aerospace and Civil Engineering, University of Manchester, UK

G. Jagadeesh

Department of Aerospace Engineering,

Indian Institute of Science, Bangalore, India

Abstract

The study of detonations and their interactions are vital for the understanding of the high-speed flow physics involved and the ultimate goal of controlling their detrimental effects. However, producing safe and repeatable detonations within the laboratory can be quite challenging, leading to the use of computational studies which ultimately require experimental data for their validation. It is the objective of the current study to examine the induced flow field from the interaction of a shock front and accompanying products of combustion, produced from the detonation taking place within a non-electrical tube lined with explosive material, with porous plates with varying porosities, 0.7% to 9.7%. State of the art high-speed schlieren photography alongside high resolution pressure measurements are used to visualise the induced flow field and examine the attenuation effects which occur at different porosities. The detonation tube is placed at different distances from the plates' surface, 0 mm to 30 mm, and the pressure at the rear of the plate is recorded and compared. The results indicate that depending on the level of porosity and the Mach number of the precursor shock front secondary reflected and transmitted shock waves are formed through the coalescence of compression waves. With reduced porosity, the plates act almost as a solid surface, therefore the shock propagates faster along its surface.

---

*k.kontis@manchester.ac.uk

I. INTRODUCTION

Implications of studying shock waves relate to the prediction, protection, and control of the overpressures obtained in these phenomena, whether they be intentionally created from explosions or due to accidents such as those occurring in the chemical or nuclear industries.[1–4] Shock-porous media interactions offer insight to fundamental flow physics related to shock reflection transition phenomena, compressible turbulence in the form of vortices and vortex sheets, and of course shock-vortex interactions.[5–9] Studying shock-porous media interactions can also be applied to understanding wave propagations during earthquakes which are in essence strong shocks travelling from beneath the earth's crust through layers of rock and soil which behave as the porous medium in this case. According to Britan et al.[10] most structures exposed to pressure loading have the ability to withstand a slower pressure rise much better than a sudden rise. They also makes the interesting suggestion of using porous media in the ventilation system of shelters due attenuate any shock waves which might travel down these passages. The control and better understanding of blasts also has applications to pulse detonation engines (PDEs)[11–14] where the combustion that takes places occurs much more rapidly and violently.

According to Hargather and Settles[15] creating the conditions for safe, controllable, and cheap explosive blasts within the laboratory is no easy feat since the majority of testing takes place outdoors with tens of kilos of explosive material in a relatively uncontrollable environment. Using NONEL tubes to create shock waves not only has the benefit of creating repeatable and safe blasts but has the added advantage of also generating the products of combustion. This allows for a more realistic analysis of the flows encountered during high-speed combustion in explosions and PDEs, which will also provide data for the validation of computational codes and analytical models.

II. EXPERIMENTAL SETUP

A. Porous plates

Three porous plates with varying levels of porosity are examined in this study. Images of these plates are provided in Figure 1. The porosity is defined as the ratio between the visible area through the plate where the flow is allowed to pass unaffected and the total plate area.

This definition eradicates the effect of plate thickness. Porosities of 9.7%, 1.9%, and 0.7% are tested with plates having thicknesses of 10 mm, 15 mm, and 25 mm, respectively. The plates are made from a metalo-ceramic alloy with honeycomb shaped voids.

B. High-speed schlieren photography

High-speed schlieren photography[16] with an optical arrangement similar to that used by Zare-Behtash et al.[17] was employed to visualise the flow, details of the apparatus can be found therein. The Shimadzu Hyper-Vision camera, capable of recording images at a rate of up to 1 Mfps, was used to create a motion picture of the flow field. Even though different frame rates were used to study some interactions, the exposure was kept at a maximum of 2 μs to ensure the flow is frozen in time. Illumination for the Shimadzu camera was provided by a 300 W continuous Xenon lamp.

C. NONEL

Non-electrical (NONEL) tubes are used in blasting and mining, crew escape systems in military aircraft, ordnance systems in launch vehicles and missiles, and the study of detonations and their interaction within the laboratory.[18] Due to the detonation of the reactants inside the plastic NONEL tube, a shock wave is created which propagates through the tube. A NONEL DynoLine tube was used in the current study having an outer diameter of 3 mm. A length of 0.3 m of NONEL tubing was used for each run.

A DynoStart 2 Spark generator with a capacitance of 0.2 μF and output voltage of 2500 V was used to initiate the detonation. Both DynoLine and DynoStart were manufactured by Dyno Nobel Sweden AB (now, Orica Mining Services). The DynoLine contains a mixture of Octogen (HMX) ($\sim$92% by weight) and traces of Aluminium ($\sim$8% by weight) at 18 mg/m length of the tube. The energy in these blast waves has been estimated to be about 1.25 J. The primary shock wave position along the axis of the tube was well described by a theory proposed by Jones.[19] This theory was proposed for blast waves of intermediate strength ($10 < \Delta p/p_0 \leq 0.02$, where Δp is the overpressure).

The shock wave created propagates along the tube and diffracts into the ambient, closely followed by the products of combustion which comprises the reaction front, as shown in

Figure 2. Shortly after the shock front leaves the NONEL, except a small region along the tube axis, the shock front decouples from the reaction zone, these zones are labelled in Figures 2(a) and (b). The decoupled reaction zone contains shocked but unreacted gases.[20] NONEL tubes were also use by Zare-Behtash et al.[21] to study 2D shock interactions.

Due to the small exit diameter of the NONEL tube, it behaves as a point source. Figure 3 depicts the primary shock wave position when viewed from three vantage points during schlieren photography: horizontal, vertical and 45 degree inclination. The fact that the points all lie on the same line concurs that the diffracted shock wave is indeed spherical in nature.

Figure 4 shows the variation of the primary shock velocity with increasing shock wave radius calculated from high-speed schlieren. Therefore by changing the distance of the NONEL relative to the plates the interaction of shock waves having different strength can be studied.

D. Pressure measurements

Figure 5 shows the setup used to measure the total pressure behind the porous plates. The transducer is placed flush with the rear surface of the plate as the NONEL tube is traversed away starting from 0 mm to 15 mm and finally 30 mm from the surface of the porous plates. The pressure was recorded at a rate of 125 kHz using a Kulite XT-190M transducer connected to a National Instruments USB-6251 data acquisition system which was controlled using LabVIEW. Every run was repeated twice and the average of the two runs was used to analyse the induced flow field.

The degree of repeatability of the pressure measurements is an indication of the repeatability of the entire system, since it takes into account the shock/flow generated by the NONEL, the subsequent interaction with the plate, and finally the measurement of the flow pressure behind the plate. This value is calculated by repeating the same run four times, calculating the average peak pressure for the runs and afterwards dividing the difference between the peak pressures and this average by the mean value of the four. This leads to an error in repeatability of approximately $\pm 3.6\%$.

III. RESULTS AND DISCUSSION

The schlieren images of Figure 6 show the flow developed when the NONEL is flush with the plates' surface. For comparison, the images are chosen so that the location of the reflected wave in each case is approximately the same. In all three cases of porosity the incident shock and products of combustion are able to penetrate the plates. With reduced porosity there is less area for the flow to penetrate, leading to greater blockage and hence accumulation of the combustion products at the front surface of the plates. As a result of the interaction between the incident shock and the pores of the plates, multiple internal reflections, diffractions, and interactions between these waves themselves occur resulting in numerous compression waves emerging from either sides of the plates. Based on the random scattering of the perforations present within the plates and the low level of porosity, it is believed that the transmitted shock wave is a result of the coalescence of these waves. As the precursor shock arrives at the surface of the porous plates, it is transmitted as a compression wave through the material whilst a shock wave is reflected backwards. From visual inspection, it is clear that with the reduction in porosity, less of the combustion products are able to pass through the plates and a build up occurs at the front edge.

Levy et al.[22] used a very simple but effective model to describe how the compression wave propagates through a porous material interacting with the rigid cell walls and arrives at the other edge. Ignoring the diffraction mechanism, their model stated that any part of the moving wave that hits the skeleton of the pore is reflected back whilst the other portions pass through. Figure 7 shows schlieren images comparing the three plates with the NONEL tube placed 15 mm from the front edge. At a distance of 15 mm the precursor shock front has a velocity of 528 ± 10 m/s (Figure 4). The distinct difference between these cases and when the NONEL is flush with the porous plate is the presence of secondary transmitted and reflected waves. Comparing these waves for the different porosity conditions, it seems that the level of porosity has a significant role in whether or not a secondary wave occurs. For example, a secondary transmitted wave is faintly visible in Figure 7(a), clearly visible in Figure 7(b), but does not occur in Figure 7(c) for the least porous plate. A similar trend occurs for the secondary reflected wave, although a distinct wave is identifiable in Figure 7(c) for the least porous plate, the same cannot be said for the most porous plate in Figure 7(a). With a reduction in porosity, a greater number of more complex internal wave interactions

5

occur within the plate. These interactions cause a decay in shock strength and the waves that manage to travel through to the other side have become much weaker to coalesce into a single front. Based on the interaction model of Levy et al,[22] due to a greater number of skeletal structure, more of the initially transmitted compression wave will reflect backwards creating the secondary reflected wave of Figure 7(c).

When the NONEL tube was moved 30 mm from the plates' surface, the velocity of the precursor shock front reduces to approximately 409±15 m/s at the surface of the plates (Figure 4). For all porosities tested, no secondary reflected or transmitted wave was observed. From Figure 8 which shows the two extreme porosity levels, as with the previous locations, the propagation of the combustion products is prohibited with reduction in porosity. The timing of these figures was chosen to allow comparison between the compression wave patterns. With greater porosity and therefore less skeletal material, a greater number of compression waves are generated, as can be seen in Figure 8(a), which propagate outwards. On the other hand, in Figure 8(b) the flow field is almost empty of any compression waves because the least porous plate produces a greater number of wave interactions, shock reflections, and diffractions, which all contribute to the weakening of these waves.

The peak total pressure measured after the shock interaction with the plates, shown in Figure 9, reveals a linear drop in pressure as the NONEL is moved further away. As expected, the plate with the highest porosity of 9.7% provides less resistance to the propagation of the transmitted compression wave leading to higher pressures. Referring back to Figure 4 where the velocity of the shock front was shown to decay with distance, the reduction in the total pressure measured after the plates is also related to the weaker incident shock impinging on the plate surface. In all cases examined, a sharp rise in pressure was captured which is indicative of a compression front travelling through the porous medium. If the compression front had decayed as it travelled through the porous plates, then a more gradual rise in pressure would have been expected.

The shock propagation Mach number along the plates' surface, determined from the schlieren images is plotted in Figure 10. In Figure 10(a), which shows the Mach number of the shock moving along the front edge of the plates, the different NONEL distances and plate surfaces do not result in any significant change in the propagation Mach number. The shock wave moving along the rear of the plate, however, in Figure 10(b) shows a different behaviour. The shock Mach number along the plate surface increases with reduced porosity. The reason

6

for the increase in shock Mach number with reduction in plate porosity is believed to be several fold: (i) since the incident shock travels through smaller openings with a reduction in porosity, its propagation speed is increased,[23] (ii) due to the smaller area available, the pressure within the plate increases, maintaining the high pressure ratio across the shock front, and (iii) the plate with the least amount of porosity acts almost as a solid plate with no grooves to decelerate the shock front.[24]

Figure 10(b) also shows that for a given porosity the shock speed along the surface increases as the NONEL is moved away from the plate. This behaviour is explained with the aid of Figure 11. As the NONEL tube is moved away from the plate, the diffracted shock wave becomes more planar as it propagates outwards and its radius increases. Since the shock has an almost planar front, the edges emerges quicker from the rear of the plate since it has less distance to travel.

IV. CONCLUSIONS

Using a non-electrical (NONEL) tube with a combination of HMX and aluminium powder reactants deposited on the internal surface, a controlled and repeatable detonation was produced. The NONEL tube acts almost as a point source, creating a spherical shock wave.

With a reduction in porosity, the propagation of the combustion products through the plate was deterred. However, the pressure measurements and schlieren visualizations indicated that a sharp compression wave travels through and emerges on the other side as a transmitted shock wave.

The influencing parameters in this study were the porosity and the distance the NONEL is placed from the plate surface which determines the precursor shock Mach number. Depending on these parameters, secondary reflected and transmitted waves occur as a result of the merger between the multiple waves created from the complex and numerous interactions taking place within the plates.

Over a longer period, the reduction in porosity created a flow field with relatively less compression waves on either side of the plate.

An interesting observation was the fact that although the Mach number of the reflected shock as it travels along the plate's surface was quite similar for the different porosity and distances examined, the Mach number of the transmitted shock along the surface was found

to increase with reduced porosity of the plate.

Acknowledgments

[1] Beavers, G.S., Matta, R.K., "Reflection of weak shock waves from permeable materials," *AIAA Journal* **10**, 959–961, (1972).

[2] Teodorczyk, A., Lee, J.H.S., "Detonation attenuation by foams and wire meshes lining the walls," *Shock Waves* **4**, 225–236, (1995).

[3] Britan, A., Karpov, A.V., Vasilev, E.I., Igra, O., Ben-Dor, G., Shapiro, E., "Experimental and numerical study of shock wave interaction with perforated plates," *Journal of Fluids Engineering* **126**, 399–409, (2004).

[4] Hargather, M.J., Settles, G.S., "Optical measurement and scaling of blasts from gram-range explosive charges," *Shock Waves* **17**, 215–223, (2007).

[5] Onodera, H., Takayama, K., "Interaction of a plane shock wave with slitted wedges," *Experiments in Fluids* **10**, 109–115, (1990).

[6] Skews, B.W., "Oblique reflection of shock waves from rigid porous materials," *Shock Waves* **4**, 145–154, (1994).

[7] Skews, B.W., Takayama, K., "Flow through a perforated surface due to shock-wave impact," *Journal of Fluid Mechanics* **314**, 27–52, (1996).

[8] Skews, B.W., "Shock wave interaction with porous plates," *Experiments in Fluids* **39**, 875–884, (2005).

[9] Kontis, K., An, R., Zare-Behtash, H., Kounadis, D., "Head-on collision of shock wave induced vortices with solid and perforated walls," *Physics of Fluids* **20**, 016104, (2008).

[10] Britan, A., Igra, O., Ben-Dor, G., Shapiro, H., "Shock wave attenuation by grids and orifice plates," *Shock Waves* **16**, 1–15, (2006).

[11] Kailasanath, K., "Recent developments in the research on pulse detonation engines,"*AIAA Journal* **41**, 145–159, (2003).

[12] Ma, F., Choi, J.Y., Yang, V., "Thrust chamber dynamics and propulsive performance of single-tube pulse detonation engines," *Journal of Propulsion and Power* **21**, 512–526 (2005).

[13] Glaser, A.J., Caldwell, N., Gutmark, E., Hoke, J., Bradley, R., Schauer, F., "Study on the operation of pulse-detonation engine-driven ejector," *Journal of Propulsion and Power*, **24**, 1324–1331 (2008).

[14] Zare-Behtash, H., Gongora-Orozco, N., Kontis, K., "Effect of primary jet geometry on ejector

performance: a cold-flow investigation," *International Journal of Heat and Fluid Flow* **32**, 596–607, (2011).

[15] Hargather, M.J., Settles, G.S., "Laboratory-scale techniques for the measurement of a material response to an explosive blast," *International Journal of Impact Engineering*, **36**, 940–947 (2008).

[16] Settles, G.S. "Schlieren and Shadowgraph techniques," *Springer Verlag* (2001).

[17] Zare-Behtash, H., Kontis, K., Gongora-Orozco, N., Takayama, K., "Compressible vortex loops: effect of nozzle geometry," *International Journal of Heat and Fluid Flow* **30**, 561–576, (2009).

[18] Yang, L.C., Do, I.H.P., "Nonelectrical tube explosive transfer system," *AIAA* **38**, 2260–2267, (2000).

[19] Jones, D.L., "Intermediate strength blast wave," *Physics of Fluids* **11**, 1664–1667, (1968).

[20] Pingten, F., Shepherd, J.E., "Detonation diffraction in gases," *Combustion and Flame* **156**, 665–677, (2009).

[21] Zare-Behtash, H., Gongora-Orozco, N., Kontis, K., Jagadeesh, G., "Study of detonation interactions inside a two-dimensional ejector using detonation transmission tubing," *Journal of Propulsion and Power* **26**, 878–882, (2010).

[22] Levy, A., Ben-Dor, G., Skews, B.W., Sorek, S., "Head-on collision of normal shock waves with rigid porous materials," *Experiments in Fluids* **15**, 183–190, (1993).

[23] Chisnell, R.F., "The motion of a shock wave in a channel, with applications to cylindrical and spherical shock waves," *Journal of Fluid Mechanics* **2**, 286–298, (1957).

[24] Gongora-Orozco, N., Zare-Behtash, H., Kontis, K., "Global unsteady pressure-sensitive paint measurements of a moving shock wave using thin-layer chromatography," *Measurement* **43**, 152–155, (2010).
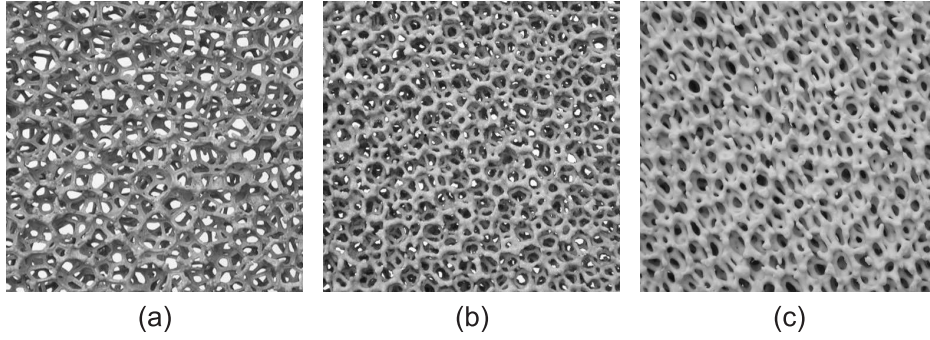
List of Figures

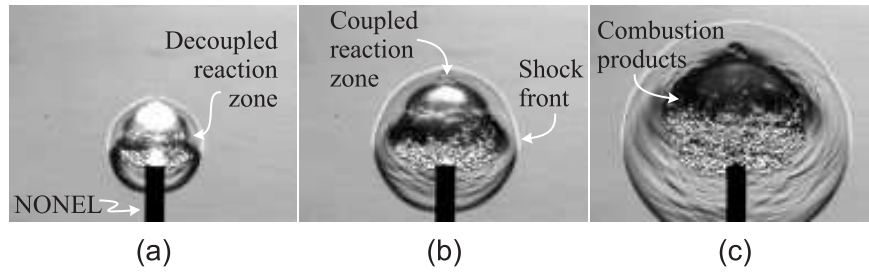FIG. 1: Photographs of the porous plates used, porosity (a) 9.7%, (b) 1.9%, (c) 0.7%.

FIG. 2: Flow created by the NONEL at t= (a) 18 μs, (b) 30 μs, (c) 52 μs after the initial emergence of the shock front.
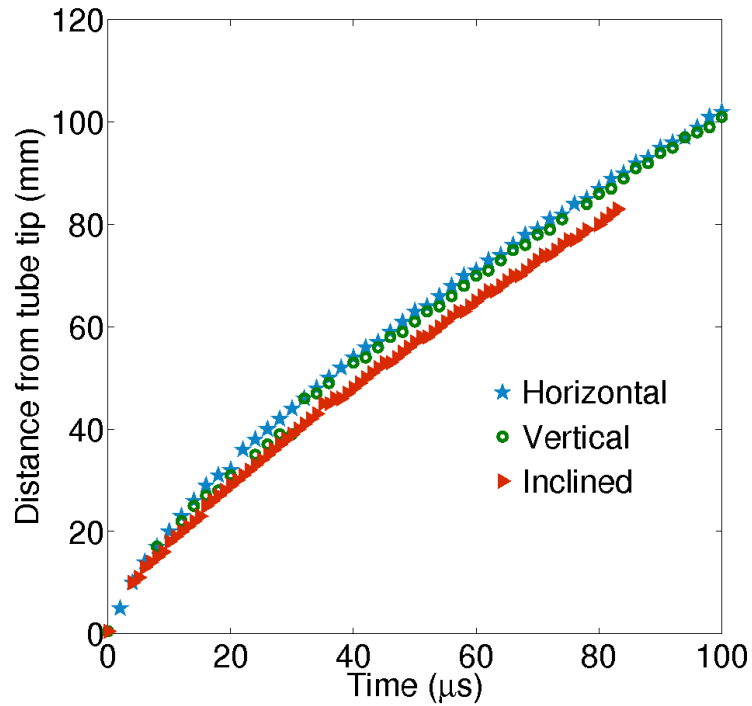

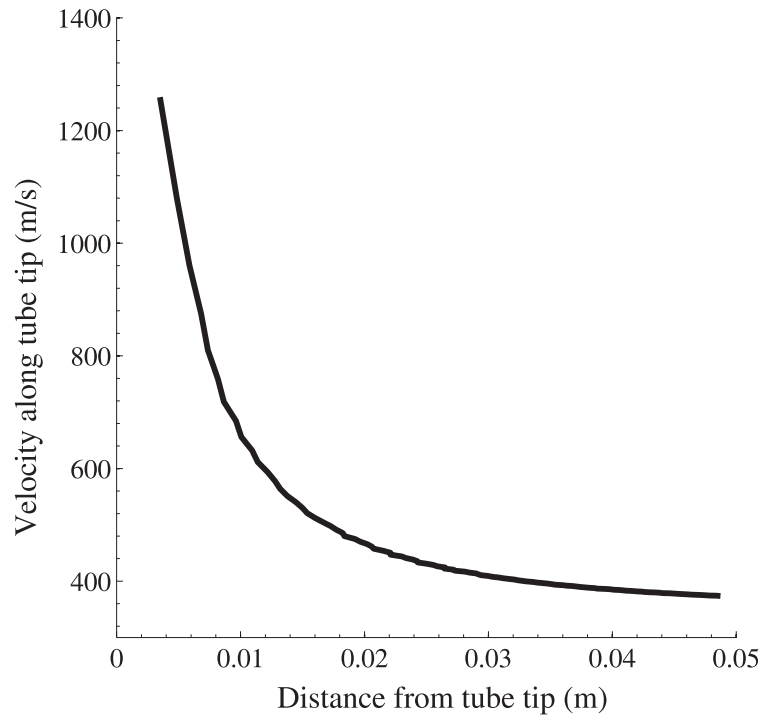FIG. 3: Position of the shock front traced from three different vantage points.

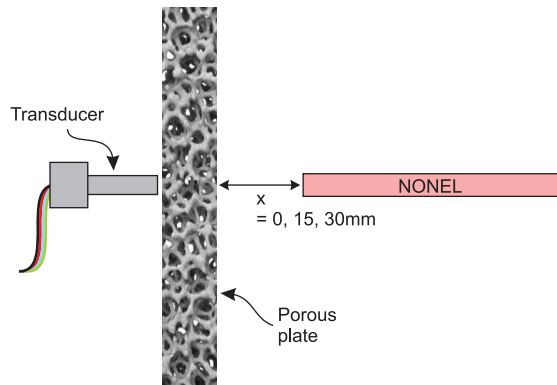FIG. 4: Primary shock wave velocity.

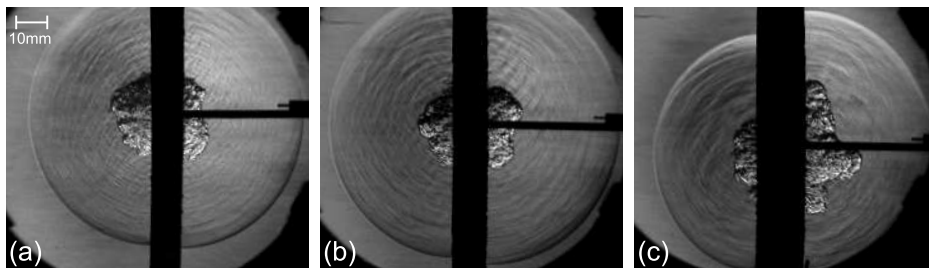FIG. 5: Experimental setup for the measurement of total pressure behind the porous plates.

FIG. 6: NONEL flushed with the plates' surface, porosity (a) 9.7%, (b) 1.9%, (c) 0.7%.

13
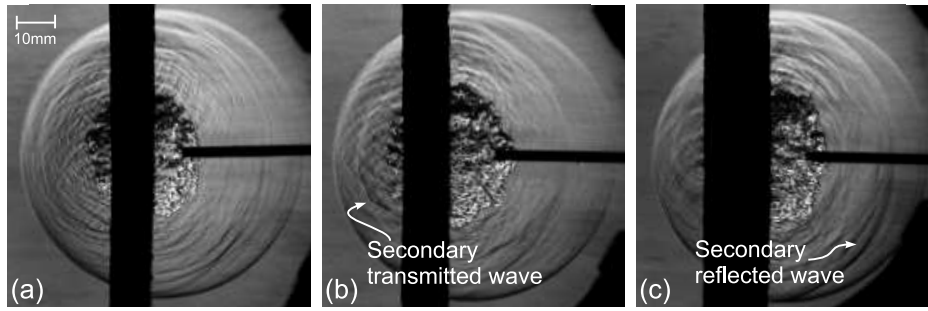
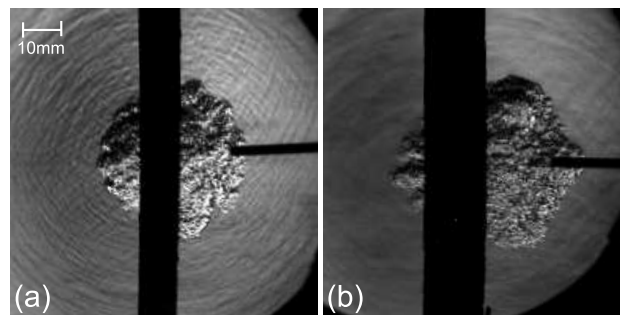FIG. 7: NONEL 15 mm from the plates' surface, porosity (a) 9.7%, (b) 1.9%, (c) 0.7%.

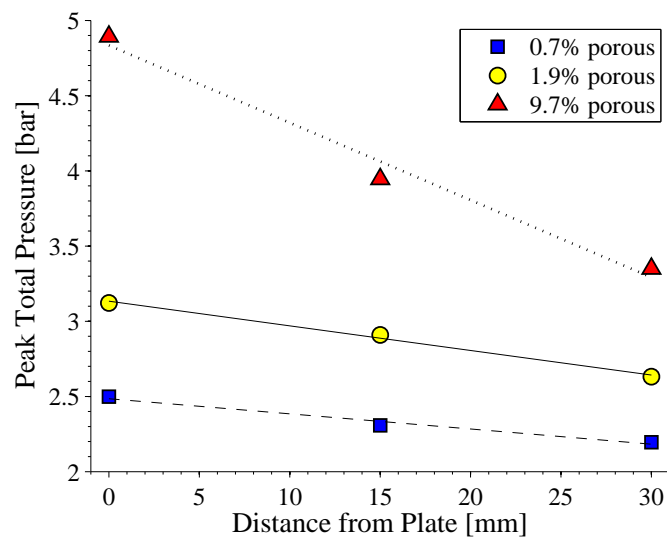FIG. 8: NONEL 30 mm from the plates' surface, porosity (a) 9.7%, (b) 0.7%.

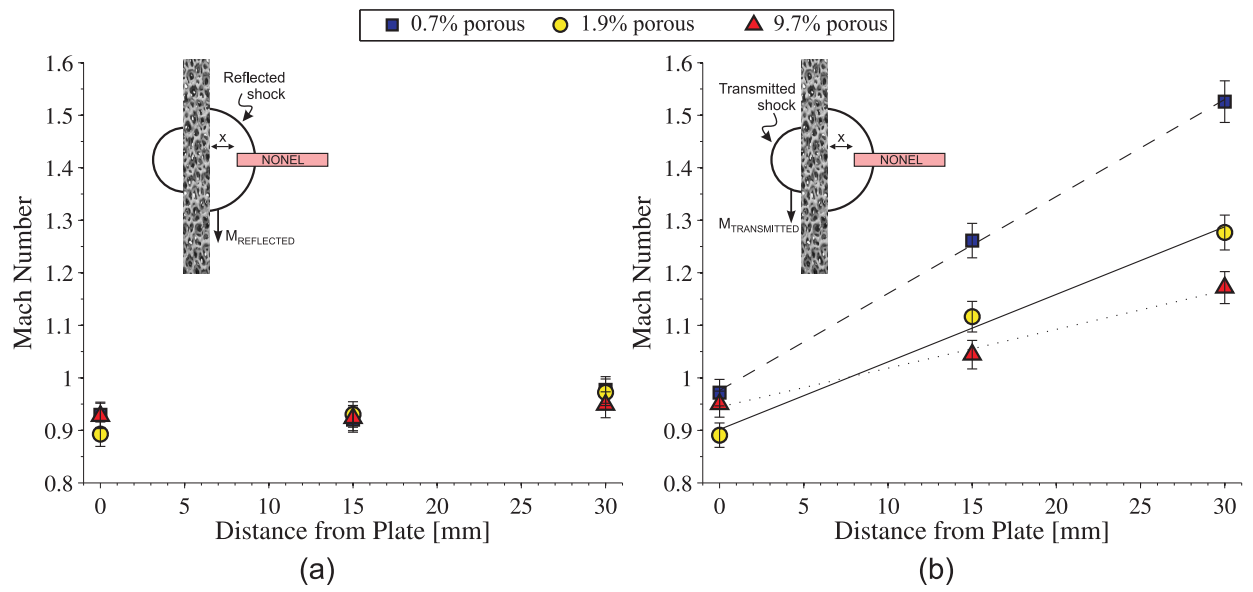FIG. 9: Peak pressure measured after the porous plate.

FIG. 10: Shock propagation Mach numbers along the plate surface for: (a) reflected shock, (b) transmitted shock.
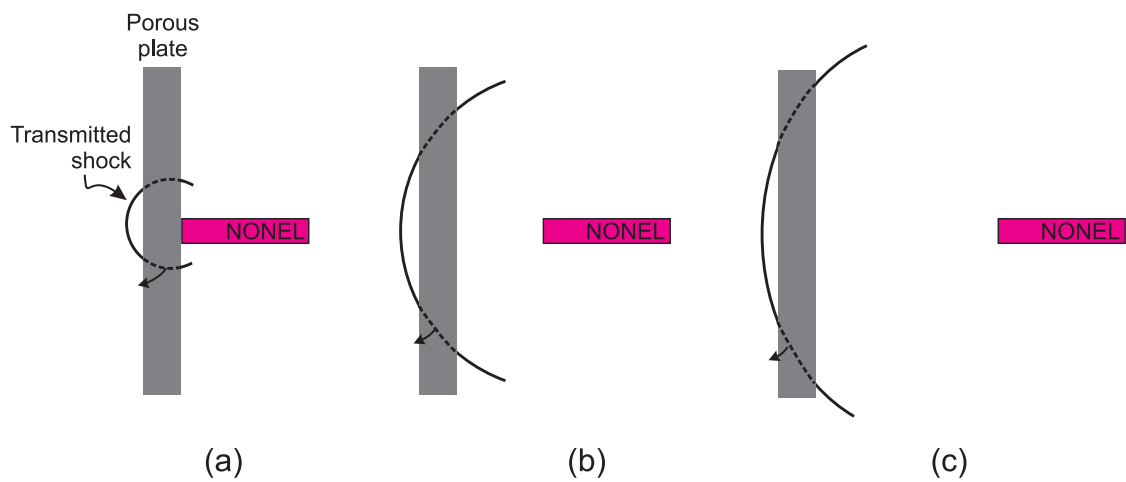

FIG. 11: Emergence of the transmitted shock at different NONEL locations: (a) flushed, (b) 15 mm, (c) 30 mm.